

Inhibition of Vascular Endothelial Growth Factor in the Primate Ovary Up-Regulates Hypoxia-Inducible Factor-1 α in the Follicle and Corpus Luteum

W. Colin Duncan, Sander van den Driesche, and Hamish M. Fraser

Division of Reproductive and Developmental Sciences (W.C.D., S.v.d.D.), University of Edinburgh EH16 4SB, United Kingdom; and Medical Research Council Human Reproductive Sciences Unit (H.M.F.), Queens Medical Research Institute, Edinburgh EH16 4TJ, United Kingdom

Vascular endothelial growth factor (VEGF)-dependent angiogenesis is crucial for follicular growth, and corpus luteum formation and function, in the primate ovary. In the ovary VEGF can be hormonally regulated, but in other systems, the main regulator of VEGF expression is hypoxia. We hypothesized that hypoxia was involved in the regulation of angiogenesis in the cycling ovary. We therefore used immunohistochemistry to localize hypoxia-inducible factor (HIF)-1 α in the marmoset ovary across the ovarian cycle. We also investigated the effect of VEGF inhibition, using VEGF Trap (aflibercept), on HIF-1 α localization during the follicular and luteal phases of the cycle. Finally, we studied the effect of chorionic gonadotropin stimulation of the corpus luteum during early pregnancy. Nuclear HIF-1 α staining was largely absent from normally growing preantral and antral follicles. However, there was marked up-regulation of nuclear HIF-1 α

in the granulosa cells at ovulation that persisted into the early corpus luteum. Mature corpora lutea and those collected during early pregnancy had minimal nuclear HIF-1 α staining. The inhibition of VEGF in the mid-luteal stage resulted in a time-dependent up-regulation of luteal nuclear HIF-1 α staining ($P < 0.05$). There was never any nuclear HIF-1 α in the theca cells of the follicle, but VEGF Trap treatment during the follicular ($P < 0.001$) or luteal ($P < 0.001$) phase increased the proportion of antral follicles with nuclear HIF-1 α staining in the granulosa cells. These results indicate that HIF-1 α is up-regulated after vascular inhibition, using VEGF Trap, in the follicle and corpus luteum. However, it is also acutely up-regulated during ovulation. This suggests a role for HIF-1 α in both hypoxic and hormonal regulation of ovarian VEGF expression *in vivo*. (*Endocrinology* 149: 3313-3320, 2008)

THE MAJOR SITE of physiological angiogenesis in the adult is the female reproductive tract, notably the ovary (1). The granulosa cells of the dominant follicle are avascular, and yet each granulosa-lutein cell of the mature corpus luteum is adjacent to an endothelial cell. Indeed endothelial cells are abundant in the corpus luteum, accounting for approximately 50% of luteal cells, and the corpus luteum has a blood supply around eight times, per unit mass, that of the kidney (1). We have shown that vascular endothelial growth factor (VEGF) is the major regulator of luteal angiogenesis in the primate ovary (2). When VEGF action is inhibited, luteal formation continues, but the resulting, poorly functioning, corpus luteum has a rudimentary vascular bed (3). We have also shown that VEGF is required for ongoing function and maintenance of the vasculature of the mature corpus luteum (4, 5).

In addition to formation of the corpus luteum, angiogenesis is required for antral follicular growth. Inhibition of VEGF in the follicular phase inhibits follicular growth and results in small, poorly vascularized antral follicles, and no large or dominant follicles develop (2, 6). Gonadotropins

have a clear role in the regulation of follicular growth and angiogenesis. Treatment with GnRH antagonists in the follicular phase also results in small, poorly vascularized, antral follicles (7). In addition, GnRH antagonist treatment in the luteal phase results in luteolysis and associated vascular regression (8).

It is therefore likely that VEGF expression is regulated by gonadotropins in the ovary. This is supported by gonadotropin up-regulation of VEGF in primary cultures of luteinized granulosa cells (9, 10) and by the marked increase in follicular fluid VEGF concentrations after the LH surge (11). In addition, the temporal changes in VEGF expression across the luteal phase, and its up-regulation by human chorionic gonadotropin (hCG) in simulated early pregnancy in women (12), also support this notion. However in other tissue systems the primary regulator of VEGF expression is hypoxia (13). Indeed, it has been reported that hypoxia, rather than gonadotropins, is the main regulator of VEGF secretion in primary cultures of luteal cells from non-human primates (14) and women (15).

The role of gonadotropins and hypoxia in the regulation of ovarian VEGF expression therefore is still not clear. Where VEGF is regulated by hypoxia, there is an up-regulation of specific transcription factors, notably hypoxia inducible factor (HIF)-1 α that is translocated from the cytoplasm to the nucleus (16, 17). We hypothesized that HIF-1 α was involved in physiological angiogenesis in the ovary and that its localization would change in different functional phases of the ovarian cycle.

First Published Online April 3, 2008

Abbreviations: hCG, Human chorionic gonadotropin; HIF, hypoxia-inducible factor; NGS, normal goat serum; PBS-T, PBS plus Tween 20; PG, prostaglandin; VEGF, vascular endothelial growth factor.

Endocrinology is published monthly by The Endocrine Society (<http://www.endo-society.org>), the foremost professional society serving the endocrine community.

We therefore investigated the localization of HIF-1 α protein in the primate ovary during the follicular and luteal phases of natural cycles. We also studied the effect of cycle manipulation on HIF-1 α localization using three strategies: 1) inhibition of VEGF in the follicular phase, that is known to up-regulate follicular VEGF expression (6), 2) inhibition of VEGF in the midluteal phase that has been shown to inhibit endothelial cell survival and vascular integrity (5), and 3) gonadotrophic stimulation of the corpus luteum in early pregnancy that in women causes an up-regulation of VEGF (12).

Materials and Methods

Animals

Adult female common marmoset monkeys (*Callithrix jacchus*) with a body weight of approximately 350 g and regular ovulatory cycles (28 d cycle length) with ovulation on d 8 were housed together with a younger sister or prepubertal female as described previously (6). Blood samples were collected three times per week by femoral venipuncture without anesthesia, and plasma was subjected to progesterone assay for the presence of ovulatory rises, as described previously (5).

Treatment

Experiments were carried out in accordance with the Animals (Scientific Procedures) Act, 1986, and were approved by the local ethical review process committee. In the first set of experiments, the follicular phase was investigated. To synchronize timing of ovulation, during the pretreatment cycle, marmosets were given 1 μ g prostaglandin (PG) F_{2 α} analog (cloprostenol, Planate; Coopers Animal Health Ltd., Crewe, UK) im in the mid- to late luteal phase (d 13–15) to induce luteolysis (6). This method of synchronizing follicular recruitment is followed by follicle selection on cycle d 5 and ovulation between d 9 and 11 (18) in which the day of synchronization is d 0.

To block VEGF, we used VEGF Trap (afibercept), a recombinant chimeric protein comprising portions of the extracellular domains of the human VEGF receptors 1 and 2 expressed in sequence with the Fc portion of human Ig (19). VEGF Trap binds all isoforms of VEGF-A, VEGF-B, and placental growth factor. Four marmosets were treated with VEGF Trap at a dose of 25 mg/kg⁻¹ injected sc at the time of PGF_{2 α} treatment (d 0), and four were treated on d 5 of the cycle (midfollicular phase). Control animals (n = 4) were treated with human Fc (25 mg/kg⁻¹ sc). Ovaries were collected on d 10. These ovaries had been used in previous studies to assess the effect of VEGF Trap on the follicle (20, 21). Ovaries from untreated marmosets on d 5 (n = 4) were also available (20).

In the second set of experiments, luteal phase administration of VEGF Trap was used. In these animals ovulation was designated luteal d 0 and defined as the day preceding a rise from follicular phase (<32 nmol/liter⁻¹) progesterone followed by a progressive increase in progesterone (5). These criteria have been used in our and other colonies to accurately identify the day of ovulation to within \pm 1 d (22). Marmosets exhibiting at least one ovulatory cycle immediately before being recruited into the study were selected. Marmosets were treated with a single injection of 25 mg/kg⁻¹ sc VEGF Trap in the midluteal phase (d 8–10). Control marmosets were treated with recombinant human Fc (25 mg/kg⁻¹ sc). Ovaries were collected 1, 2, and 4 d (n = 4 per group) later (5). Control animal ovaries (n = 4 per group) were collected 2, 4, and 8 d later. These ovaries have been investigated in a previous study assessing inhibition of luteal VEGF in the postangiogenic window (5).

In a third set of experiments, ovaries from pregnant marmosets were investigated. These ovaries have been collected and studied as part of a previous investigation into the rescued corpus luteum of the marmoset (23). At the time of PGF_{2 α} administration, a fertile male was introduced, and marmosets were killed 28 d after ovulation and confirmed pregnant by the presence of trophoblast in serial sections of the uterus and plasma levels of chorionic gonadotropin of greater than 20 ng/ml⁻¹ (23).

Collection of ovaries

Animals were sedated and humanely killed as described previously (5, 6). In the luteal phase, the corpora lutea were identified macroscopically and ovaries bisected along the line of maximal luteal area before fixation in 4% (vol/vol) neutral buffered formalin (Van Waters and Rogers International Ltd., Leicestershire, UK). After 24 h, the ovaries were transferred into 70% (vol/vol) ethanol, dehydrated, and embedded in paraffin according to standard procedures.

Immunohistochemistry

To facilitate classification of follicular health, cell death was determined by immunohistochemistry for caspase-3 as described previously (5). A specific rabbit polyclonal antibody was used for the immunolocalization of HIF-1 α (clone H-206; Santa Cruz Biotechnology, Santa Cruz, CA) using 5- μ m paraffin tissue sections of marmoset ovaries prepared on poly-L-lysine-coated microscope slides. These sections were dewaxed, rehydrated, washed in PBS, subjected to antigen retrieval by boiling in a pressure cooker in 0.01 mol/liter⁻¹ citric acid (pH 6.0) for 5 min, and left to cool to room temperature. All sections were washed and placed in 3% (vol/vol) H₂O₂/methanol for 30 min, followed by an avidin and biotin block (Vector Laboratories, Peterborough, UK) and a further block using normal goat serum (NGS; Diagnostics Scotland, Edinburgh, UK) diluted 1:5 in PBS containing 5% (wt/vol) BSA (NGS/PBS/BSA) for 1 h at room temperature. Sections were incubated overnight in primary antibody diluted 1:100 in NGS/PBS/BSA at 4 C.

All sections were then washed twice for 5 min in PBS plus 0.01% (vol/vol) Tween 20 (PBS-T; Sigma-Aldrich, Poole, UK) before incubation with biotinylated goat antirabbit secondary antibody (Dako Corp., Cambridge, UK), diluted 1:500 in NGS/PBS/BSA. Incubation lasted for 1 h and was followed by two washes in PBS-T for 5 min. Thereafter sections were incubated in avidin-biotin complex-horseradish peroxidase (Vector Laboratories) for 1 h according to the manufacturer's instructions. All sections were washed in PBS-T (2 \times 5 min) and bound antibodies visualized by incubation with liquid 3,3'-diaminobenzidine tetrahydrochloride (Dako). Sections were counterstained lightly with hematoxylin to enable cell identification. Negative controls for each antibody examined were performed identically to the above protocol with the primary antibody omitted or replaced with nonspecific Igs (Santa Cruz Biotechnology). Images were captured using a Provis microscope (Olympus Corp. Optical Co., London, UK) equipped with a DCS330 camera (Eastman Kodak Co., Rochester, NY), stored on a computer (Hewlett-Packard, Portland, OR), and assembled using Photoshop 7.0.1 (Adobe Systems Inc., Mountain View, CA).

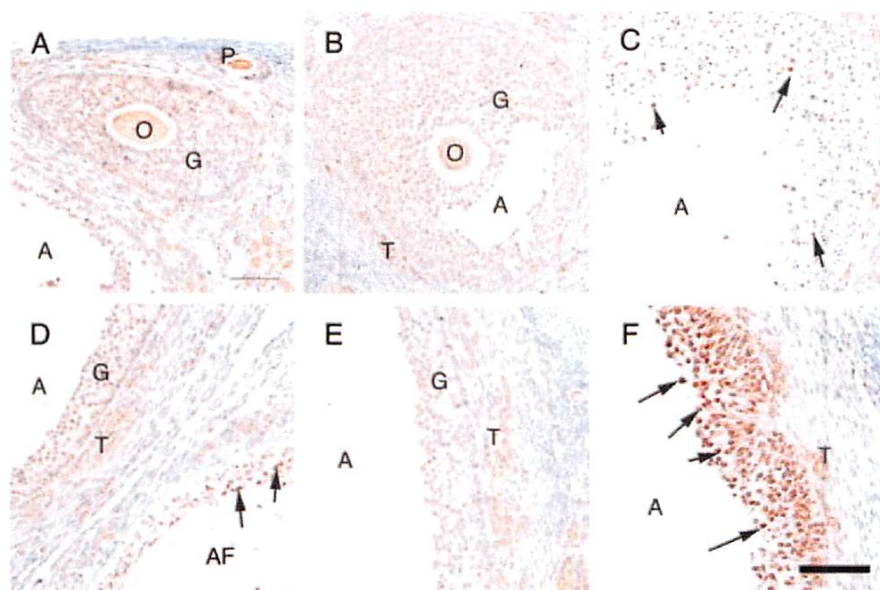
Analysis of sections

Sections were analyzed by an observer blinded to treatment type. For the analysis of corpora lutea, the percentage of luteal steroidogenic cells with clear nuclear HIF-1 α immunostaining was recorded using a stratified random sampling technique (24). Both ovaries were examined for each animal, but where there was more than one corpus luteum, the score was averaged for that animal before statistical analysis. For the analysis of follicular granulosa cell HIF-1 α immunostaining, all antral follicles (<1 mm in size) (25) in midline sections of both ovaries were counted and classified as positive where there was marked nuclear HIF-1 α staining in the all the granulosa cells, negative where no clear nuclear immunostaining could be detected in any granulosa cells, or intermediate where there was patchy or faint nuclear HIF-1 α staining in the granulosa cells.

Statistical analysis

The percentage of nuclear HIF-1 α stained steroidogenic cells in corpora lutea was analyzed using the Kruskal-Wallis test. The proportion of immunostained antral follicles, in the follicular and luteal phases after treatments, was analyzed using a χ^2 test. Statistical differences where $P < 0.05$ were considered significant.

FIG. 1. Immunolocalization of HIF-1 α in the marmoset follicle. A, Preantral follicle in the marmoset ovary with neighboring primary (P) and antral follicle (A). B, Antral follicle in different ovary showing light cytoplasmic HIF-1 α staining in various follicular cell types. C, Atretic follicle showing specific patchy nuclear staining for HIF-1 α (arrows). D, Follicular phase ovary with selected antral (A) follicle with no staining with a neighboring atretic follicle (AF) demonstrating clear nuclear HIF-1 α immunostaining in the granulosa cells layer (arrows). E, Pre-ovulatory dominant follicle showing no nuclear HIF-1 α immunostaining. F, Luteinizing follicle during ovulation demonstrating intense nuclear HIF-1 α staining in the granulosa cells (arrows). O, Oocyte; G, granulosa cells layer; T, theca cell layer; A, antral cavity. Scale bar, 100 μ m.



Results

HIF-1 α localization in the follicle

In the normal follicular phase, there was light HIF-1 α immunostaining in the cytoplasm of cells of the developing follicle, including the oocyte, theca cells, and granulosa cells (Fig. 1). There was no clear nuclear HIF-1 α localization in preantral (Fig. 1A), antral (Fig. 1B), selected (Fig. 1D), or dominant follicles (Fig. 1E) in all ovaries and follicles examined. However, in atretic follicles, nuclear HIF-1 α immunostaining could clearly be detected in the granulosa cell layer (Fig. 1, C and D) in all tissue sections examined. Although there was no nuclear localization of HIF-1 α in the preovulatory follicle (Fig. 1E), ovulation was associated with intense nuclear HIF-1 α staining in all granulosa cells (Fig. 1F).

The effect of VEGF inhibition on follicular HIF-1 α localization

After exposure to VEGF Trap in the follicular phase, the light cytoplasmic staining of the oocyte and primordial, primary (Fig. 2A), and secondary (Fig. 2B) follicles seen in control ovaries was maintained. Nuclear immunostaining could not be detected in any follicles of these stages. No staining could be detected in negative control sections (Fig. 2, C and I). However, in larger preantral follicles, nuclear HIF-1 α expression could now be detected in some granulosa cells (Fig. 2D). However, the most marked change was the appearance of antral follicles with marked nuclear staining in the granulosa cell layer (Fig. 2E). In contrast, antral follicles from control ovaries showed minimal nuclear HIF-1 α localization (Fig. 2F).

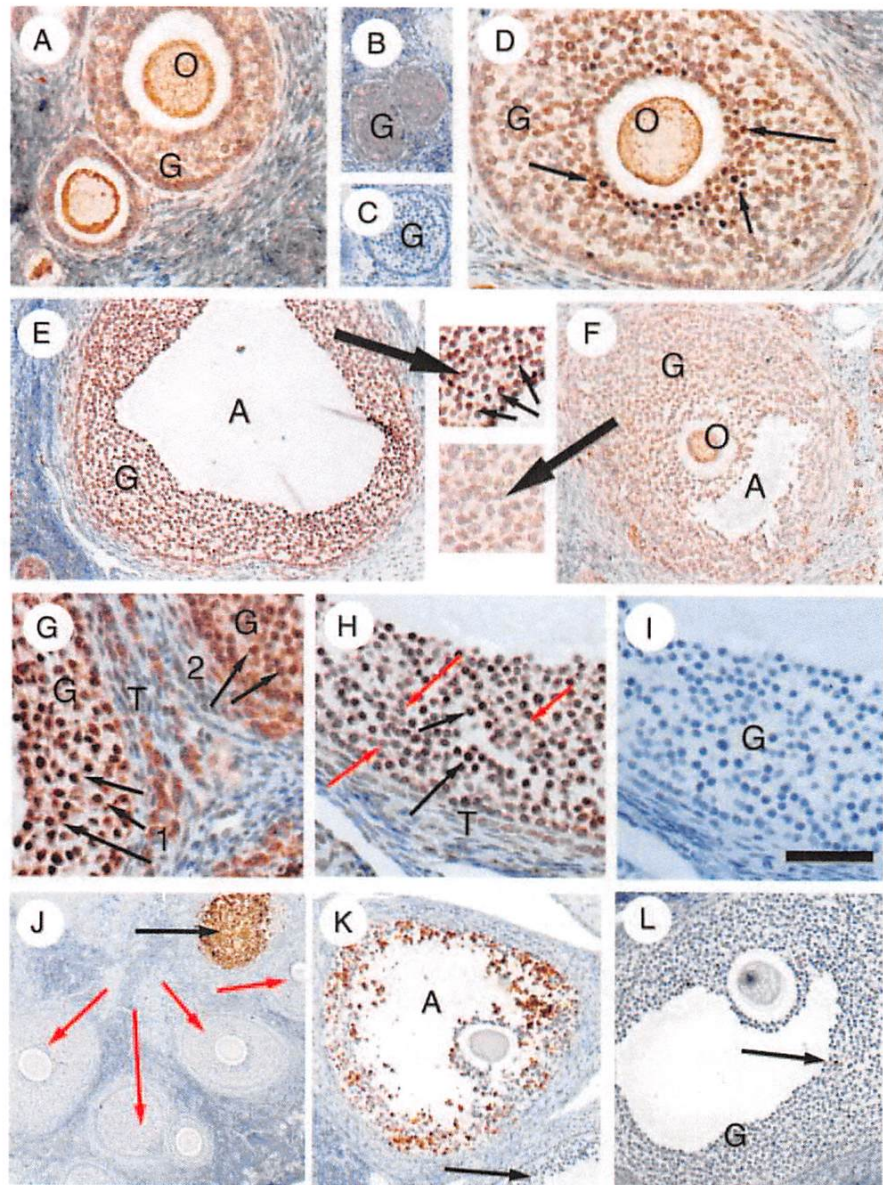
Where nuclear HIF-1 α immunostaining was seen, there were two apparent patterns: intense staining in all granulosa cells (Fig. 2, E and G) or light (Fig. 2G), patchy (Fig. 2H) staining in the granulosa cell layer. Because atresia is associated with increase HIF-1 α immunostaining, atretic follicles were identified by immunostaining serial sections for

caspase-3 (Fig. 2, J and K) and excluded from analysis. The effect of VEGF Trap treatment on the proportion of morphologically healthy antral follicles, with no or minimal (Fig. 2L) caspase-3 staining, showing intense (+), light patchy (\pm) or no staining (–) was therefore assessed (Fig. 3A). Inhibition of VEGF in the follicular phase increased the proportion of follicles with nuclear HIF-1 α staining in the granulosa cells ($P < 0.001$). Treatment with Trap from d 5 to 10 of the follicular phase was associated with more marked nuclear staining than treatment from d 0–10 of the follicular phase ($P < 0.05$) (Fig. 3A). There was also an effect of Trap treatment during the luteal phase on follicular nuclear HIF-1 α immunostaining (Fig. 3B). The proportion of antral follicles with nuclear HIF-1 α staining increased with duration of Trap treatment ($P < 0.001$) (Fig. 3B). Although there was clear nuclear staining in the granulosa cells of follicles after Trap treatment, there was never any clear nuclear staining of the theca cells of these follicles (Fig. 2, G and H). Like the atretic follicles of control ovaries, atretic follicles after VEGF Trap treatment showed patchy nuclear HIF-1 α immunostaining in granulosa cells.

HIF-1 α localization during luteal formation and regression

There was intense nuclear HIF-1 α immunostaining in the luteinizing granulosa cells, but not the theca cells, in the periovulatory period (Fig. 4A). As the follicle collapses and the corpus luteum begins to form, nuclear HIF-1 α immunostaining in the granulosa cells is maintained (Fig. 4B). However, nuclear staining was minimal in every fully formed corpora lutea examined. In the natural cycle, there was only light cytoplasmic staining of the steroidogenic cells (Fig. 4C) of corpora lutea from the mid and late-luteal phases. During natural luteolysis, cytoplasmic HIF-1 α staining of the steroidogenic cells was evident (Fig. 4D). Although in some sections of regressing corpora lutea, there was the occasional cell demonstrating possible nuclear localization of HIF-1 α , these

FIG. 2. Immunolocalization of HIF-1 α in marmoset follicles after exposure to VEGF Trap. **A**, Primordial and primary follicle in marmoset ovary after exposure to VEGF Trap from d 0 to 10 of the cycle. **B**, Small secondary follicle after the same follicular phase VEGF Trap treatment showing no nuclear HIF-1 α staining. **C**, Serial negative control section of **B**. **D**, Larger preantral follicle after Trap exposure from d 5 to 10 showing some nuclear HIF-1 α staining (*arrows*). **E**, Antral follicle, with high-power detail, in another animal after VEGF Trap treatment from d 5 to 10 of the cycle showing uniform nuclear immunostaining (*arrows*) (+). **F**, Antral follicle in follicular phase control ovary, with high-power detail, showing no nuclear HIF-1 α localization (–). **G**, High-power detail of follicles after 4 d of VEGF Trap treatment in the luteal phase showing marked nuclear staining in granulosa cells (*arrows*) of follicle 1 (+) and lighter, more patchy, staining (\pm) in neighboring follicle 2, but not in theca cells or either follicle. **H**, Follicle after Trap treatment from d 5 to 10 showing the patchy staining pattern in which some granulosa cells (*black arrows*) show nuclear staining, but others (*red arrows*) do not. **I**, Serial negative control section of **H**. **J**, Caspase-3 immunostaining of preantral follicles demonstrating one atretic (*black arrow*) and four healthy follicles (*red arrows*). **K**, Caspase-3 immunostaining of antral follicle confirming atresia with no staining of neighboring antral follicle (*arrow*). **L**, Caspase-3 staining of healthy antral follicle showing a single atretic cell (*arrow*). O, Oocyte; G, granulosa cell; T, theca cell; A, antral cavity. Scale bar, 150 μ m (E, F, and J–L) and 100 μ m (A–D and G–I).



cells were very infrequent (Fig. 4D). There was no specific immunostaining in the negative control sections (Fig. 4E).

The effect of VEGF inhibition on luteal HIF-1 α localization

Nuclear HIF-1 α immunostaining was only rarely detected in the steroidogenic cells of fully functional mid- to late luteal corpora lutea (Fig. 5A). *In vivo* exposure to VEGF Trap in the midluteal phase was associated with the appearance of clear nuclear HIF-1 α staining in some steroidogenic cells (Fig. 5, B–D). The proportion of steroidogenic cells with nuclear HIF-1 α expression increased with the duration of exposure to VEGF Trap ($P < 0.05$) (Fig. 6). There was never any specific staining in negative control sections (Fig. 5E), in addition to nuclear staining in steroidogenic cells after Trap treatment,

nuclear HIF-1 α expression was evident in some luteal endothelial cells (Fig. 5F). Endothelial cells never showed nuclear HIF-1 α localization in the corpus luteum in the absence of VEGF Trap treatment. Exposure to chorionic gonadotropin during early pregnancy did not result in an increased proportion of luteal cells with nuclear HIF-1 α staining than that seen in the functional corpus luteum of control cycles (Fig. 6).

Discussion

HIF-1 α is a transcription factor involved in the hypoxic regulation of VEGF expression (26). Its action is associated with nuclear localization of the protein, and as such, nuclear immunolocalization of the protein has been shown to be predictive of hypoxic signaling in tissues in which angio-

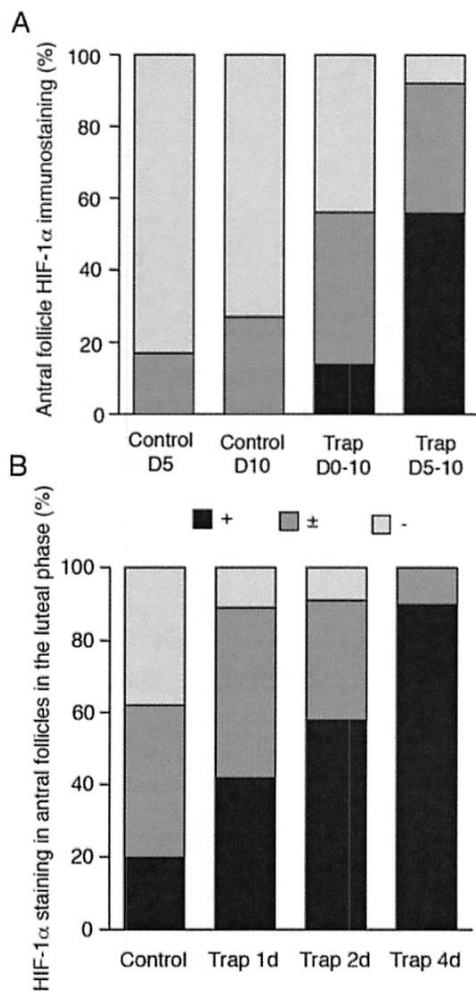


FIG. 3. HIF-1 α immunostaining in the granulosa cells of antral follicles (<1 mm). The nuclear HIF-1 α immunostaining pattern for each follicle was classified as intense in all granulosa cells (+), light or patchy in granulosa cells (\pm), or absent from granulosa cells (-). **A**, The immunostaining pattern changes after VEGF Trap treatment in the follicular phase ($P < 0.001$, χ^2). All healthy follicles in control ovaries collected in the midfollicular phase (d 5) ($n = 77$), the late follicular periovulatory phase (d 10) ($n = 26$), and from VEGF Trap-treated ovaries at d 10 after 10 d (d 0–10) ($n = 36$) or 5 d (d 5–10) ($n = 36$) of treatment were scored. **B**, The immunostaining pattern changes after VEGF treatment in the midluteal phase ($P < 0.001$, χ^2). All healthy follicles in luteal d 12 and 14 control ovaries ($n = 90$) and after VEGF Trap from luteal d 10 for 1 (1d) ($n = 45$), 2 (2d) ($n = 33$), and 4 (4d) ($n = 20$) days of treatment were scored.

genesis is required such as prostatic cancer (27) and the endometrium (16). The ovary has marked, regulated, and cyclical angiogenesis (2) that is fundamental for follicle growth (6) and luteal formation and function (4, 28). This angiogenesis is dependent on and regulated by gonadotropins (7) and VEGF (2). Here we investigated tissue hypoxia in the primate ovary by studying the nuclear localization of the HIF-1 α protein in the natural cycle and after VEGF inhibition. The change in its nuclear immunolocalization across

the natural ovarian cycle supports a role for HIF-1 α in the regulation of physiological ovarian angiogenesis.

During the follicular phase, nuclear HIF-1 α immunostaining was largely absent from the steroidogenic cells of the follicle. Indeed nuclear HIF-1 α staining was notably absent from the avascular granulosa cells of the dominant preovulatory follicle, although notably at this stage, there is clear VEGF expression in the granulosa cells (7). During ovulation there was marked HIF-1 α staining in the luteinizing granulosa cells. This immunostaining persisted into the early corpus luteum, a time during which there is intense angiogenesis that is regulated by VEGF (2). Indeed, we have previously shown that VEGF mRNA is also highly expressed at this time and reduced when LH is removed using GnRH antagonist treatment (7). These observations are consistent with periovulatory hypoxia and a possible role for the HIF-1 α transcription factor in the regulation of the intense angiogenesis associated with luteal formation. There is little previous work on HIF-1 α localization in the ovary. In the pig ovary HIF-1 α mRNA was found in corpora lutea, and expression tended to decrease as the corpus luteum matured (29). Again this is consistent with a role for HIF-1 α in luteal formation.

The clear and coordinated changes in HIF-1 α localization during ovulation would, however, also be consistent with HIF-1 α localization being hormonally regulated. In addition to hypoxia (17), HIF-1 α expression can be ligand-stimulated under nonhypoxic conditions (30). It is therefore possible that HIF-1 α is directly stimulated by the LH surge as well as the local hypoxic environment. Whether this is a direct LH effect or secondary to the increased metabolic demands and glucose use induced by LH, and required for the marked change in steroidogenesis associated with luteinization, is not clear. What is clear is that there is a link between HIF expression and the energy requirements of the cell (31). That said, the large metabolic demands of the steroidogenic cells are maintained in the functioning corpus luteum, with its fully formed vascular network, in the absence of nuclear HIF-1 α staining. This suggests that there is an associated hypoxia during luteal formation but that this signal is facilitated, and regulated, by LH. Indeed, FSH has been shown to induce HIF-1 in rat granulosa cells (32). In addition, there is evidence that HIF-2 α expression in human luteinizing granulosa cells can be directly regulated by hCG *in vitro* under normoxic conditions (33).

Outside the periovulatory period, however, the nuclear localization of HIF-1 α in the natural ovarian cycle is less marked. One time when VEGF is clearly required is in development of the follicular vasculature (2) and in the developing primate follicle, the main source of VEGF during follicular growth is the avascular granulosa cells of the follicle (6). Although there was occasional nuclear staining in the follicles of the follicular phase, this was not particularly notable despite clear VEGF expression (2). These cells, however, have the capacity to demonstrate nuclear HIF-1 α localization when VEGF is withdrawn. Whether, in the presence of VEGF, HIF-1 α expression is important but transient such that nuclear localization is difficult to detect is not yet clear. Although hypoxia may have a role in follicular development, these studies, however, would suggest that HIF-1 α -independ-

Explore Litigation Insights

Docket Alarm provides insights to develop a more informed litigation strategy and the peace of mind of knowing you're on top of things.

Real-Time Litigation Alerts



Keep your litigation team up-to-date with **real-time alerts** and advanced team management tools built for the enterprise, all while greatly reducing PACER spend.

Our comprehensive service means we can handle Federal, State, and Administrative courts across the country.

Advanced Docket Research



With over 230 million records, Docket Alarm's cloud-native docket research platform finds what other services can't. Coverage includes Federal, State, plus PTAB, TTAB, ITC and NLRB decisions, all in one place.

Identify arguments that have been successful in the past with full text, pinpoint searching. Link to case law cited within any court document via Fastcase.

Analytics At Your Fingertips



Learn what happened the last time a particular judge, opposing counsel or company faced cases similar to yours.

Advanced out-of-the-box PTAB and TTAB analytics are always at your fingertips.

API

Docket Alarm offers a powerful API (application programming interface) to developers that want to integrate case filings into their apps.

LAW FIRMS

Build custom dashboards for your attorneys and clients with live data direct from the court.

Automate many repetitive legal tasks like conflict checks, document management, and marketing.

FINANCIAL INSTITUTIONS

Litigation and bankruptcy checks for companies and debtors.

E-DISCOVERY AND LEGAL VENDORS

Sync your system to PACER to automate legal marketing.